The Astrophysical Journal, 810:99 (11pp), 2015 September 10 doi:10.1088/0004-637X/810/2/99

EVOLUTION OF A DWARF SATELLITE GALAXY EMBEDDED IN A SCALAR FIELD DARK MATTER HALO

Victor H. Robles[1], V. Lora[2], T. Matos[1], and F. J. Sánchez-Salcedo[3]
[1] Departamento de Física, Centro de Investigación y de Estudios Avanzados del IPN, 07000 D.F., México; vrobles@fis.cinvestav.mx
[2] Astronomisches Rechen-Institut, Zentrum für Astronomie der Universität Heidelberg, Mönchhofstr. 12-14, D-69120 Heidelberg, Germany; vlora@ari.uni-heidelberg.de
[3] Instituto de Astronomía, Universidad Nacional Autónoma de México, AP 70-264, 04510 D.F., México
Received 2014 October 17; accepted 2015 June 28; published 2015 September 3

ABSTRACT

The cold dark matter (CDM) model has two unsolved issues: simulations overpredict the satellite abundance around the Milky Way (MW) and it disagrees with observations of the central densities of dwarf galaxies which prefer constant density (core) profiles. One alternative explanation known as the scalar field dark matter (SFDM) model, assumes that dark matter is a scalar field of mass ($\sim 10^{-22}\,\mathrm{eV}/c^2$); this model can reduce the overabundance issue due to the lack of halo formation below a mass scale of $\sim 10^8 M_\odot$ and successfully fits the density distribution in dwarfs. One of the attractive features of the model is predicting core profiles in halos, although the determination of the core sizes is set by fitting the observational data. We perform *N*-body simulations to explore the influence of tidal forces over a stellar distribution embedded in an SFDM halo orbiting a MW-like SFDM host halo with a disk. Our simulations intend to test the viability of SFDM as an alternative model by comparing the tidal effects that result in this paradigm with those obtained in the CDM for similar mass halos. We found that galaxies in subhalos with core profiles and high central densities survive for 10 Gyr. The same occurs for galaxies in low density subhalos located far from the host disk influence, whereas satellites in low density DM halos and in tight orbits can eventually be stripped of stars. We conclude that SFDM shows consistency with results from the CDM for dwarf galaxies, but naturally offer a possibility to solve the missing satellite problem.

Key words: galaxies: dwarf – galaxies: evolution – galaxies: formation – galaxies: halos – galaxies: stellar content

1. INTRODUCTION

The lambda cold dark matter (ΛCDM) paradigm has been very successful in explaining structure formation on large scales. One of its predictions is a universal density profile for dark matter halos. Navarro et al. (1997, NFW) suggested a simple formula to describe these density profiles, which presents a divergent inner profile ($\rho(r) \propto r^{-1}$) (Diemand et al. 2005). Another prediction of the ΛCDM model is the number of subhalos per unit mass around the host galaxy. Both predictions have been challenged on scales of dwarf galaxies. In fact, a significant fraction of the rotation curves of low surface brightness (LSB) galaxies and dwarf irregular galaxies are better fitted using dark halos with a density core ($\rho(r) \propto r^0$) (Gentile et al. 2004; Wilkinson et al. 2004; Strigari et al. 2006; de Blok et al. 2008; Oh et al. 2008; Trachternach et al. 2008; Walker & Peñarrubia 2011; Agnello & Evans 2012; Peñarrubia et al. 2012; Salucci et al. 2012; Lora et al. 2013 Read et al. 2006). However, the case for cores in Milky Way (MW) satellites is still debated. For instance, Strigari et al. (2014) mentioned that the data of the Sculptor dwarf spheroidal are consistent when an NFW dark matter halo is assumed. Moreover, for dwarf galaxies in the field or Andromeda the information is about the dark matter mass and not the density profiles, so a direct determination of the slope in the density profile is not possible. Regarding the prediction in the number of subhalos, it turns out that the standard CDM model overpredicts the number of dwarf satellite galaxies in the MW and M31. This disagreement is usually referred to as the "missing satellite problem" (Klypin et al. 1999; Moore et al. 1999; Simon & Geha 2007; Belokurov et al. 2010; Macciò et al. 2012; Garrison-Kimmel et al. 2014b; Goerdt et al. 2007). Although the detection of ultra faint galaxies within the MW halo has reduced the missing satellite problem (e.g., Simon & Geha 2007), a recent study by Ibata et al. (2014) of the distribution of satellites around the MW and M31 suggests they have specific alignments forming planes that are not found in current CDM simulations. Independently of this potential issue, the central densities of MW dSph galaxies are required to be significantly lower than the densities of the largest subhalos found in collisionless DM simulations to agree with current data (Boylan-Kolchin et al. 2011; Garrison-Kimmel et al. 2014a). Indeed, CDM simulations of the Aquarius Project (Navarro et al. 2010) suggest that the MW size halos should inhabit at least eight subhalos with maximum circular velocities exceeding $30\,\mathrm{km\,s^{-1}}$, while observations indicate that only three satellite galaxies of the MW possess halos with maximum circular velocities $>30\,\mathrm{km\,s^{-1}}$. This discrepancy is known as the "too big to fail" problem.

It has been argued that the physics of baryons must be included in order to make a fair interpretation of observations on scales of MW subhalos. For instance, mass outflows given by supernova explosions could transform a cusp into a core in some field dSph galaxies at the present time. The missing satellite discrepancy may be explained as a consequence of gas reionization that quenched the star formation in halos with maximum circular velocity less than $20\,\mathrm{km\,s^{-1}}$, leaving hundreds of small mass halos without stars (Boylan-Kolchin et al. 2014). In principle using gravitational lensing techniques could confirm the existence of these dark matter halos. However, there is still no consensus on whether mass outflows and reionization can explain the observed properties of the MW satellite galaxies (Okamoto et al. 2008; Peñarrubia et al. 2012). Additionally, it seems there could be a numerical code dependence when interpreting the results obtained from simulations (Scannapieco et al. 2001, 2012).

More recently, it was noted that CDM predicts massive subhalos with central densities higher than those found in

satellite galaxies, meaning that there are DM subhalos that are massive but host no satellite galaxies (Boylan-Kolchin et al. 2011; Rashkov et al. 2012; Tollerud et al. 2012). All these problems might be related and share a common solution. The way they are correlated usually depends on the dark model paradigm (Donnino et al. 2013; Rocha et al. 2013), or gravity model (Milgrom 2010; McGaugh & Milgrom 2013), but a general fact is that solving one of these issues provides clues to the solution for the other issues. It it worth mentioning that although supernovae explosions seem to play a crucial role in forming cores in field dwarf galaxies and more massive systems where the gas is recycled to continue the star formation (Mashchenko et al. 2008; Brook et al. 2011; Governato et al. 2010, 2012; Pontzen & Governato 2012; Garrison-Kimmel et al. 2013), it is unclear that the same feedback implementation works in satellite galaxies where the gas content is negligible and their stellar populations are mostly dominated by old stars. In this sense, dark matter models where the core formation is through DM properties and not by the specifics of astrophysical processes are still viable alternative solutions.

One of these alternative models is the scalar field dark matter (SFDM) model. The idea was first considered by Sin (1994) and independently introduced by Guzmán & Matos (2000). In the SFDM model the main hypothesis is that dark matter is a self-interacting real scalar field of small mass ($m \sim 10^{-22}\,\mathrm{eV}/c^2$) that condensates forming Bose–Einstein condensate (BEC) "drops" (Lora et al. 2012; Magaña et al. 2012a). We interpret these BEC drops as the halos of galaxies (Matos & Ureña-López 2001) such that the DM wave properties and the Heisenberg uncertainty principle stop the DM phase-space density from growing indefinitely. These properties automatically avoid the divergent density (cuspy) profiles in DM halos and reduce the number of small satellites due to the mass cut-off in the power spectrum (Hu et al. 2000; Marsh & Silk 2014). For this typical mass, it follows that the critical temperature of condensation of the scalar field is $T_{\mathrm{crit}} \sim m^{-5/3} \sim$ TeV, thus, BEC drops can be formed very early in the universe. There have also been numerous studies that analyzed the behavior of the scalar field at large scales (Berezhiani et al. 1992; Hu et al. 2000; Matos & Ureña-López 2001, 2007; Harko & Madarassy 2011; Suárez & Matos 2011; Chavanis 2012; Magaña et al. 2012b; Suárez et al. 2014), concluding that it reproduces the successes of the CDM model at those scales.

One straightforward and universal prediction of the wave properties of this model is that DM halos have core profiles since their initial formation (Robles & Matos 2013a; Suárez et al. 2014). If halo distributions are flat from the beginning, then strong feedback blowouts are not required to produce low density distributions in DM-dominated systems. Some other consequences of this particular feature have been explored in different contexts; to fit rotation curves in LSB and dwarf galaxies (Harko & Madarassy 2011; Chavanis 2012; Lora et al. 2012; Robles & Matos 2013a; Lora & Magaña 2014) and to make strong lensing analyses (González-Morales et al. 2013; Robles & Matos 2013b).

All these successes of the model have motivated us to test the model further in order to know if it can be regarded as a serious DM candidate in the universe; conducting these tests is necessary for models whose DM properties are quite different from those of the standard classical particle description. Thus, here we study the evolution of the stellar component of satellite dwarf galaxies embedded in SFDM halos orbiting within an SFDM MW-sized host halo. Our study provides constraints on both the final stellar distribution of dSphs and the survival of faint or ultra faint systems.

We pursue this task by studying the conditions under which tidal disruption may occur in the SFDM model. Previous studies have shown, using empirical core-like density profiles for DM halos, that tidal disruption can be more important than in halos with NFW profiles, especially if they pass close to the galactic disk (see Klimentowski et al. 2009 and Peñarrubia et al. 2010 for collisionless simulations). However, until now there have not been studies addressing whether the tidal effects are strong enough to completely remove the stars in classical and ultra faint dwarf galaxies hosted by BEC halos. The present work aims to investigate this issue through a series of simulations of a stellar component described by a Plummer profile when it is embedded in an SFDM subhalo subject to the influence of an SFDM host halo with a disk component. We also conducted simulations without the disk to compare its effect on the stars.

The article is organized as follows: in Section 2 we explain the SFDM model and present the density profiles to be used in the simulations. Section 3 describes the simulations, Section 4 contains our results and discussions of the satellite galaxy evolution, and Section 5 presents our conclusions.

2. THE BARYONIC COMPONENTS

2.1. The dSph Stellar Component

The dSph galaxies have low luminosities ($L_V \sim 10^2$–$10^7 L_\odot$) and very large dynamical mass-to-light ratios ($M/L) \gtrsim 10$, which translate into a large amount of DM (Muñoz et al. 2005; Strigari et al. 2006; Gilmore et al. 2007; Mateo et al. 2008; Walker et al. 2009; Wolf et al. 2010; McGaugh et al. 2010). Nevertheless, we detect the galaxies because of the stars and, in fact, using them as tracers of the potential gives us information about their potential well. Here we use a Plummer density profile (Plummer 1911) for the stellar component of the dSph, where the mass density profile is given by

$$\rho(r) = \frac{3M_*}{4\pi r_{\mathrm{p}}^3}\left(1 + \frac{r}{r_{\mathrm{p}}}\right)^{-5/2}, \tag{1}$$

where M_* is the mass of the stellar component, and r_{p} is the Plummer radius. One should note that r_{p} can be related to the half-mass-radius r_{h} through $r_{\mathrm{h}} = 1.3 r_{\mathrm{p}}$. In our simulations, we have set a half-mass-radius of 200 pc and a stellar mass of $M_* \simeq 7.3 \times 10^5\, M_\odot$, motivated by the typical values for Draco, which is one of the classical dSph galaxies and also one of the least luminous satellites (e.g., see Martin et al. 2008 and Odenkirchen et al. 2001, for Draco).

2.2. The MW Disk Component

In some of our simulations we include the potential of the MW's baryonic disk, which we model with a Miyamoto–Nagai potential (Miyamoto & Nagai 1975)

$$\Phi_{\mathrm{d}}(R, z) = -\frac{GM_{\mathrm{d}}}{\sqrt{R^2 + \left(a + \sqrt{z^2 + b^2}\right)^2}}. \tag{2}$$

In the latter equation, M_{d} stands for the mass of the disk, and a and b stand for the horizontal and vertical scalelengths,

respectively. We have set the mass of the disk to $M_{\rm d} = 7.7 \times 10^{10} M_{\odot}$, and the scalelengths to $a = 6\,{\rm kpc}$ and $b = 0.3\,{\rm kpc}$.

2.3. The Dark Matter Component

2.3.1. The dSph DM Component

If DM is composed of scalar particles with masses $m \ll 1\ {\rm eV}/c^2$, the galactic halos have very large occupation numbers and the field behaves as a classical field that obeys the Klein–Gordon equation. For SFDM halos, the Newtonian limit is enough to describe them. From the fits to the rotation curves of DM-dominated systems, it has been found that the SFDM halos of DM-dominated galaxies are well described with the ground state (Guzmán & Ureña-López 2006; Böhmer & Harko 2007; Robles & Matos 2012; Martinez-Medina & Matos 2014). However, the larger the galaxy the more important are the effects of the non-condensed states on the mass profile. The latter means that galaxies that have RC that remains flat even at large radii are better described by adding the excited state contiributions (Bernal et al. 2010; Robles & Matos 2013a). This suggests that excited states are relevant for describing MW-sized systems. Their relevance in dwarfs is out of the scope of this work but see, for instance, Martinez-Medina et al. (2015). In this work we will then consider the base state to describe the dwarf DM halos.

Following the hypotheses mentioned above for the SF and using the temperature corrections to one loop for the scalar field, Robles & Matos (2013a) found that after the phase transition that happens in the early universe, the field rolls down to a new minimum of the potential and reaches those values where it will remain. The structures will grow and eventually form the SF halos. Assuming the field is at the minimum, the authors derive an analytical solution for a static spherical configuration that allows the presence of excited states.[4] What they found is that for an SFDM halo in the state j its density profile is given by

$$\rho_j(r) = \rho_{0,j} \frac{\sin^2\left(k_j r\right)}{\left(k_j r\right)^2}. \tag{3}$$

In the latter equation, $\rho_{0,j}$ is the central mass density, $k_j \equiv j\pi/R_{\rm h}$, j is a positive integer that identifies the minimum excited state needed to fit the data of a galaxy, $R_{\rm h}$ is a scalelength that is determined from observations and is a free parameter; fitting data for a given galaxy provides values for both parameters, the scale $R_{\rm h}$ and the central density, and the same occurs using Equation (6) but for its own parameters. There is not observational evidence that determines how far the halo should extend, but we do expect that halos spread at least enough to cover up to the outermost measured data. It follows that if galaxies have stellar distributions mostly concentrated in the center with possibly some gas surrounding them, then $R_{\rm h}$ would be larger than the radius where most of the stars are confined. Based on the trend from the fits of works that use SFDM halos (Harko & Madarassy 2011; Lora et al. 2012; Robles & Matos 2012, 2013a) where the scale radius complies with the above condition, we may take the $R_{\rm h}$ to be a truncation radius such that $\rho(r) = 0$ for $r > R_{\rm h}$ and for all $r \leqslant R_{\rm h}$ the density is given by Equation (3).

We recall that scalar field configurations in excited states are characterized by nodes, thus, for a bounded configuration the ground state has no nodes and corresponds to $j = 1$; the first excited state has one node and it is associated with $j = 2$, the second has two nodes, and so on. We remark that from this interpretation, if we are dealing with a field configuration in the ground state corresponding to zero nodes, then Equation (3) has no oscillatory behavior; only those configurations in excited states have oscillations.

From Equation (3) we obtain the mass and rotation curve velocity profiles given by

$$M(r) = \frac{4\pi\rho_{0,j}}{k_j^2}\frac{r}{2}\left(1 - \frac{\sin\left(2k_j r\right)}{2k_j r}\right), \tag{4}$$

$$V^2(r) = \frac{4\pi G\rho_{0,j}}{2k_j^2}\left(1 - \frac{\sin\left(2k_j r\right)}{2k_j r}\right), \tag{5}$$

respectively. Diez-Tejedor et al. (2014) reported that MW dSphs that are within SFDM halos in the ground state are well described with truncation radii in the range ∼0.5–2 kpc, they mentioned that a common value larger than 5 kpc is disfavored by the dynamics of dSphs provided they are in SFDM halos where only the ground state is taken into account. Martinez-Medina et al. (2015) extended this result to account for higher energy states of the scalar field in the associated SFDM halos of the MW dSphs and found that the stellar distribution lies inside the region where the ground state of the SF is mostly confined (∼0.5–1.5 kpc); also, the presence of the first excited state does not substantially affect the innermost dark matter configuration but it does allow for the possibility of a larger truncation radius (∼5 kpc). Nevertheless current data in the dwarfs analyzed are insufficient to conclude the existence of other states in SFDM halos of MW dSphs and hence determining precisely the halo radius. For our generic analysis of a typical dwarf we will then consider a value of $R_{\rm h} = 2\,{\rm kpc}$ consistent with the results suggested by the above independent analyses, additionally, note that most of the stellar component resides inside 1 kpc in most dSphs, where the dark matter distribution is not substantially modified by the precise halo radius that is considered as shown in Martinez-Medina et al. (2015).

For the parameters of the dwarf DM halo we then adopt the values $j = 1$ and a typical radius of $R_{\rm h} = 2\,{\rm kpc}$. Note that for the base state $j = 1$ there is no oscillatory behavior in the RC (Figure 1) contrary to the case with excited states (Figure 2).

For the dwarf central density ($\rho_{0,1}$), we select two different values that encompass the range of masses found in dwarfs, $0.16\,M_{\odot}\,{\rm pc}^{-3}$ (model A) and a less massive one with $0.031\,M_{\odot}\,{\rm pc}^{-3}$ (model B).

In Figure 1, the dashed lines show the circular velocity, mass, and density associated with the SFDM halos of models A (blue) and B (cyan). The corresponding SFDM dwarf core radius (defined as the radius at which the central density drops by a factor of two) is ∼750 pc for both models A and B and its presence is a distinctive prediction of the model.

[4] We refer the reader to the mentioned work for details on the calculation of the density profile of a SFDM halo given that the mathematical details are already described in that work.

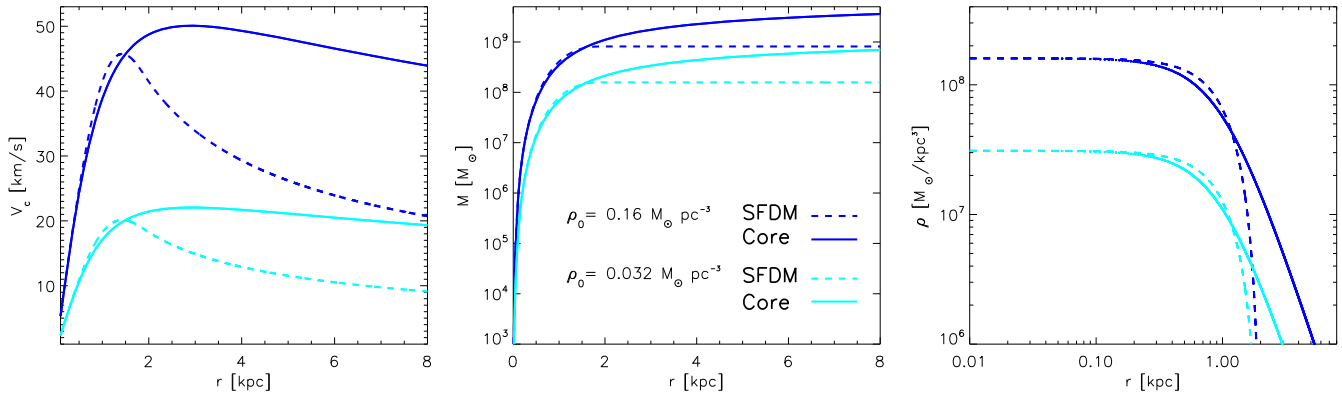

Figure 1. Circular velocity (left), mass (center), and density profile (right) associated with the two SFDM halos of the dwarf galaxy (dashed blue line) is model A: 0.16 $M_\odot$ pc^{-3}, and the dashed cyan line is model B: 0.031 $M_\odot$ pc^{-3}. The corresponding core DM models are shown with solid lines with their respective colors for comparison.

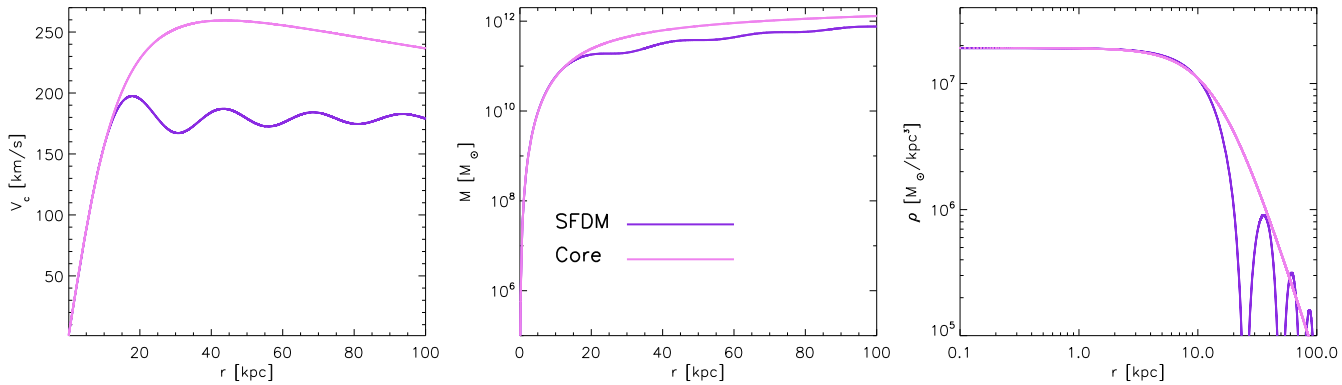

Figure 2. From left to right are the cicular velocity, mass, and density profiles used for: the MW's SFDM halo model (purple lines), and the cored DM halo (pink lines).

To compare the SFDM profiles with other cored profiles, we also consider the following profile (Peñarrubia et al. 2010)

$$\rho(r) = \frac{\rho_0}{\left(1 + \left(r/R_s\right)^2\right)^{3/2}}. \quad (6)$$

For both models A and B, we set the scale radius to $R_s = 1$ kpc (see solid lines in Figure 1).

For our mass models, the mass of the dark halo enclosed at $R_h = 2$ kpc lies in the range 10^8–$10^9 M_\odot$. The resulting M/L represent DM-dominated dSphs. For instance, the M/L of dSphs ($[M/L]_{half}$) in the MW range from $\sim 7\, M_\odot/L_\odot$ (Leo I, Fornax) to $\sim(10^3)\, M_\odot/L_\odot$ (UMa II, Seg, UMaI) (Collins et al. 2014). In particular, Draco has a very low luminosity but a high estimated total mass within the tidal radius of $M(r_t) = 2.2$–$3.5 \times 10^7\, M_\odot$ (Odenkirchen et al. 2001); this leads to a high M/L of $(M/L)_i \simeq 92$–146 (Irwin & Hatzidimitriou 1995; Armandroff et al. 1995).

2.3.2. The MW DM Component

In the SFDM model, the fluctuations are expected to grow faster than in the standard model (Suárez & Matos 2011), implying that galaxies are fully formed at large redshifts. In fact, some recent high redshift observations suggest the existence of well formed galaxies very early in the universe (Collins et al. 2009; Finkelstein et al. 2013; Charles et al. 2014). From the results of hydrodynamical CDM simulations that model the MW, one sees that its dark and luminous matter have not substantially changed since $z \lesssim 2$ ($\sim$10 Gyr ago) (Governato et al. 2007; Klimentowski et al. 2009; Peñarrubia et al. 2010; Kassin et al. 2012; Diemand et al. 2007). Then, for the initial conditions, we can assume a host with similar parameters that reproduces current MW data. We found that using $\rho_{0,4} = 0.0191\, M_\odot\, \mathrm{pc}^{-3}$, $j = 4$, and $R_h = 100$ kpc (see purple lines in Figure 2) in Equation (3) gives a good representation of the MW DM in the SFDM model. Although a detailed analysis of the MW with an SFDM is out of the scope of this work, we obtained the quoted values following the usual procedure of estimating the parameters that model our neighborhood, that is, we search the parameters consistent with the circular velocity in the solar neighborhood and the Oort constants, and we find a velocity of $\sim 200\, \mathrm{km\, s^{-1}}$ at 8.5 kpc and constants $A = 15.5\, \mathrm{km\, s^{-1}\, kpc^{-1}}$ and $B = -14.4\, \mathrm{km\, s^{-1}\, kpc^{-1}}$, similar to results from previous works (Feast & Whitelock 1997). We did the estimation when the disk was present and obtained the above values for the SFDM halo and the disk parameters reported following Equation (2).

For the MW's cored DM profile (Equation (6)), we set $R_s = 15$ kpc. The corresponding circular velocity, mass, and density of the cored DM halo are shown with pink lines in Figure 2. It has to be noted that, for both (SFDM and cored) MW halos, the core radius is $\sim$11.5 kpc and that the mass estimations within 100 kpc are comparable. Therefore, the DM profiles are not identical but the total mass enclosed at the halo radius is the same. Given that all our satellites have orbits inside this radius, we choose $R_h = 100$ kpc, principally because

our main focus is to study the tidal stripping of the stellar component of these satellites, whose apocenters never become larger than 100 kpc during the simulation. As the MW dark matter mass outside this radius is not essential to our study we can truncate the halo at that point; it then follows a Keplerian decay for larger radii. The wiggles found in the halo and shown in Figure 2 are also a particular difference of this SFDM profile with respect to other core models.

3. SIMULATIONS

We simulate the evolution of the stellar component of the dwarf galaxy, which is embedded in a rigid SFDM halo potential using the *N*-body code SUPERBOX (Fellhauer et al. 2000). SUPERBOX is a highly efficient particle-mesh, collisionless-dynamics code with high resolution sub-grids. In our case, SUPERBOX uses three nested grids centered in the density center of the dwarf galaxy. We used 128^3 cubic cells for each of the grids. The inner grid is meant to resolve the inner region of the dwarf galaxy. The spatial resolution is determined by the number of grid cells per dimension (N_c) and the grid radius ($r_{\rm grid}$). Then the side length of one grid cell is defined as $l = \frac{2r_{\rm grid}}{N_c - 4}$. For $N_c = 128$, the resolution is 0.5 pc. SUPERBOX integrates the equations of motion with a leap-frog algorithm and a constant time step of dt. We selected a time step of $dt = 1$ Myr in our simulations.

For the orbit of the dwarf galaxy, we assume an apocenter distance from the MW, $r_{\rm a} = 70$ kpc (Bonanos et al. 2004), and two different pericenter distances ($r_{\rm p} = 14$ and 35 kpc). We conducted simulations with and without adding the presence of a Miyamoto–Nagai disk in the MW potential to assess the effects on the dwarfs due to the close encounter with the disk component. Our main interest is the stellar component evolution which is located deep inside the subhalo. Peñarrubia et al. (2010) show that the major effect of tidal disruption of a DM suhalo occurs in the outermost radius, while inner regions ($\lesssim$1 kpc) are less affected by tides and the density profiles are only shifted to a slightly lower value maintaining the same inner shape during the evolution. The evolution changes if the subhalo's pericenter is smaller than the length of the disk in the event that this component is present, meaning that when the subhalo effectively cross through the disk several times it can lose a considerable amount of its initial mass or even get destroyed if the orbit's pericenter is $\sim$1.8 kpc, however, these are rare events. Given these results and that we consider rigid subhalos, we focus our analyses on orbits with pericenters larger than the disk scalelength avoiding direct collisions with the disk that would require a live subhalo. Since stars serve as tracers of the subhalo potential, any major tidal disruption of the stars would be indicative of a substantial change in the evolution of the subhalo. In such cases, a live halo would be needed. This happens only in one of our simulations and will not be used to draw the overall conclusions of this work. However, it does serve to show that our results are consistent with those in Peñarrubia et al. (2010).

In our first couple of simulations, denoted by A1 and B1, the dwarf galaxy is embedded in the MW SFDM halo potential without including the baryonic MW disk component (first two rows of Figure 3). The dwarf galaxy is placed at a galactocentric distance of 70 kpc and orbits in the $x-y$ plane with $r_{\rm p}/r_{\rm a} = 1/2$.

In the second pair of simulations, A2 and B2, we model the dwarf galaxy embedded in the MW SFDM halo potential in a circular orbit ($r_{\rm p}/r_{\rm a} = 1$), including the baryonic MW disk component (see last two rows of Figure 3).

In the third pair of simulations, A3 and B3, we model the dwarf galaxy embedded in the MW SFDM halo potential, with $r_{\rm p}/r_{\rm a} = 1/2$, but now we include a rigid baryonic MW disk component. We rerun these two simulations to compare with the empirical profile (Equation (6)) referred to as $\rm A3_{core}$ and $\rm B3_{core}$.

We observe from Figures 3 and 4 that the dwarf galaxy survives unperturbed for $\sim$10 Gyr in models A1−B3. Moreover, from models A1, A3, B1, and B3, we observe that there is a negligible effect of the MW's baryonic disk on the dwarfs that are in SFDM subhalos.

The fourth pair of simulations, named A4 and B4, resembles cases 3 but with $r_{\rm p}/r_{\rm a} = 1/5$ (A4 and B4 are in Figures 4 and 5). For model A4, the stellar component of the dwarf galaxy remains undisturbed, while the B4 model shows a major star mass loss. We run an extra couple of simulations for completeness as discussed in the next section. Table 1 summarizes all our simulations.

4. RESULTS AND DISCUSSION

Figure 6 shows the dwarf galaxy stellar mass profile at $t = 0$ and $t = 10$ Gyr in all our simulations. From the upper left panel in Figure 6 we see that all A models lose some particles, but the loss is not substantial and the galaxies survive with essentially the same initial mass after 10 Gyr. These simulations suggest that the density is high enough to strongly bind the stars and prevent the disruption of the satellite. A similar behavior is seen when a cuspy-like profile is used (Klimentowski et al. 2009; Łokas et al. 2012), making tidal disruption an inefficient process in both core and cusp-like subhalos to reduce their stellar mass within 1 kpc and therefore it is not the relevant mechanism that decreases the abundance of massive dwarf satellites around MW-type galaxies, even for orbits with close pericenters of 14 kpc.

The B models for the SFDM halo show a slightly larger particle loss than the A models (upper right panel in Figure 6) except for model B4 which shows a more pronounced particle loss. The small central density of the SFDM dwarf subhalo plays a crucial role in its survival. The final mass (at $t = 10$ Gyr) for B models is smaller than the high A density model in all cases. This shows that even if the orbit is far from the MW disk, whenever the DM subhalos have low densities the stars in the center are susceptible to spread out more than in denser halos as seen by comparing the two upper panels in Figure 6 within 500 pc.

One of the features that is seen from the stellar mass profiles is that the stars are not heavily stripped from the dwarf SFDM halo (excluding model B4). This is reassuring as it implies the DM density profile is also not strongly modified in that region and may be approximated by a fixed halo profile for orbits without small pericenters. The result is strengthened with the findings of Peñarrubia et al. (2010) for live subhalos with $r_{\rm p}/r_{\rm a} = 1/2$ and a core DM profile; even in the presence of a live disk the DM subhalos remain almost the same in the central region after 10 Gyr. Hence, the tidal effects on the subhalo are small within 1 kpc, which is about the relevant core size of our simulated subhalo. Therefore we consider that our approximation of an SFDM rigid halo is

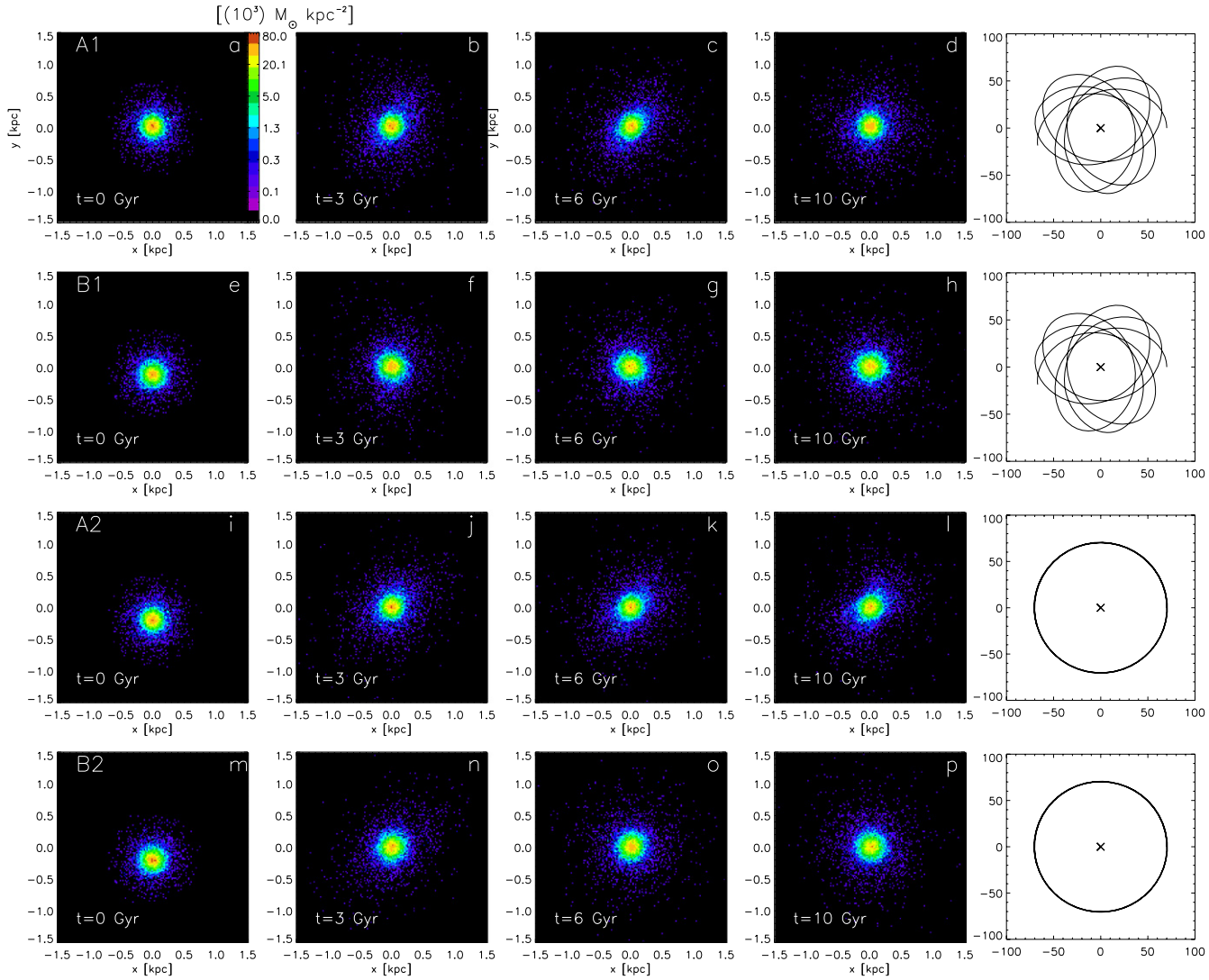

Figure 3. Surface mass density of the dwarf galaxy for models A1, B1, A2, and B2 for $t = 0$, 3, 6, and 10 Gyr; all plots are centered in the dwarf galaxy. In the last column, we show the orbit of the satellite galaxy around a Milky Way SFDM halo.

sufficient as long as the subhalos do not get well inside the disk of the host halo.

Simulations $A3_{core}$ and $A4_{core}$ present a behavior similar to their SFDM counterparts (see the upper left panel of Figure 6). In these cases the stars in the outskirts get stripped more easily, moving to larger radii and, at the same time, causing the inner stars to redistribute to a new configuration that follows the background DM halo potential. For cases A, the potential well is deep enough that only a few stars are lost; most of them remain within 1 kpc and keep the same initial profile.

The $B3_{core}$ model has lost more mass than its analog B3 (see the upper right panel of Figure 6). This is due to the slight difference in the tail of the subhalo mass profile ($r > 2$ kpc) and the fact that the potential is not as deep as in cases A, making it easier for the tidal forces to change the central stellar distribution. From Figure 1 we note that subhalos with a core profile have a non-zero density for $r > 2$ kpc. For smaller r_p:r_a the tidal stripping and the interaction with the disk become stronger, especially for the stars in the outermost radius which are more easily stripped. In fact, given that the subhalo in $B3_{core}$ is more extended than in B3, more stars are likely to get pulled toward the tail of the halo but remain inside the subhalo. In this process the now outer stars drag some of the inner stars toward outer radii producing a more extended stellar distribution than in B3, reducing at the same time the stellar mass as shown in Figure 6.

The same occurs for the $B4_{core}$ model and its counterpart B4 (see empty and full squares in Figure 6). However, the considerable disruption in both B4 simulations indicates the need to include the disruption of the halo. In our simulations, the satellites still remain due to the assumption of a fixed subhalo, but we expect the dwarf halos to fully disrupt and that their stars get dispersed around the MW halo.

We also conducted a couple of simulations (A5 and B5) where we set the dwarf galaxy embedded in the MW SFDM halo potential with $r_p/r_a = 1/5$ including the baryonic MW disk component and similar to A4 and B4 models, but now we place the dwarf galaxy in an orbit inclined 45° from the $x-y$ plane. In this case we observe that the dwarf galaxy gets destroyed within ∼1.5 Gyr. This suggests that orbits with close pericenter distances and inclination effects are factors important to the survival of low density SFDM dwarf satellites.

In order to address the dependence of our results on the stellar mass we conducted the following two pairs of

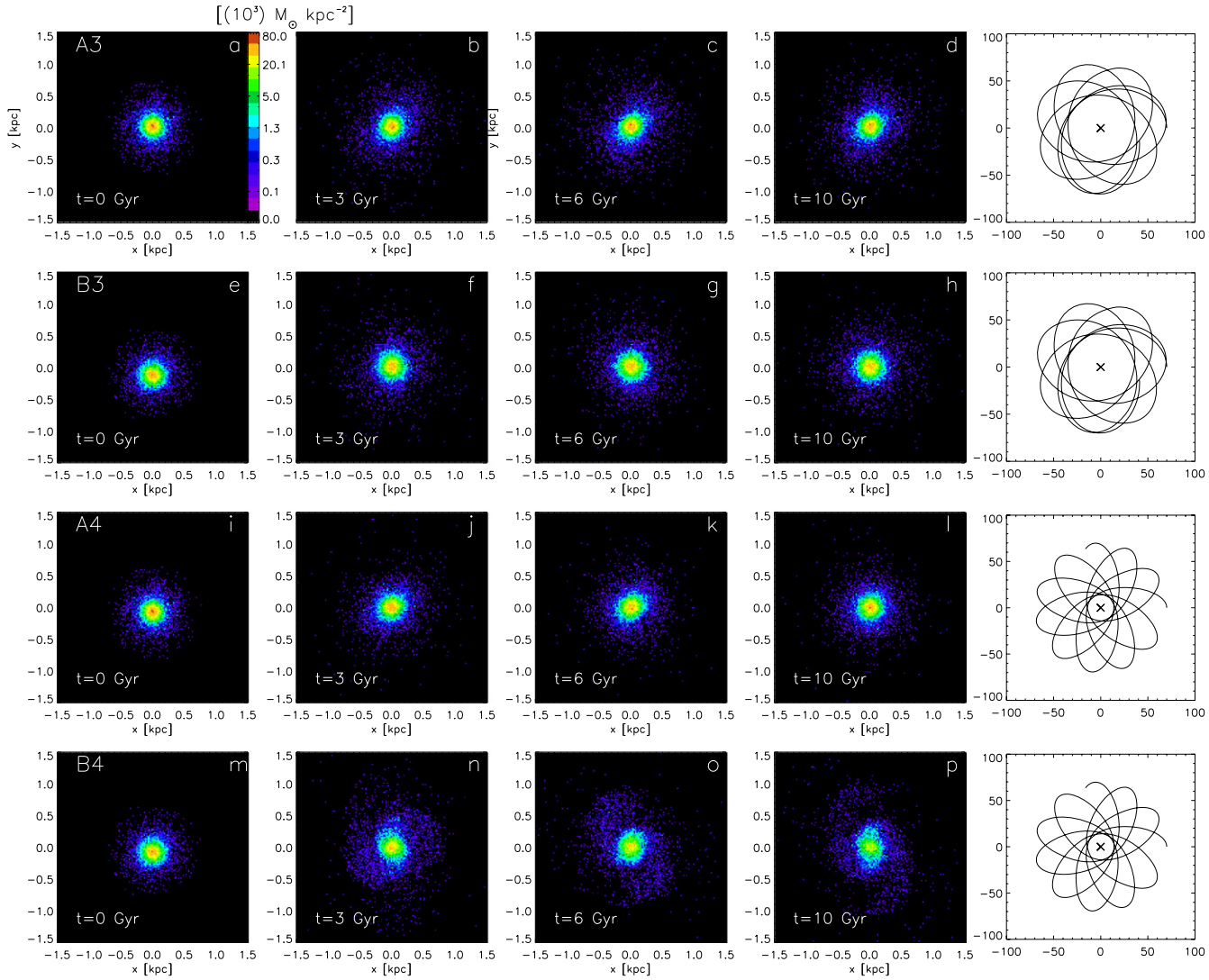

Figure 4. Same as Figure 3, but for models A3−B4.

simulations. In A6 and A6$_{\rm core}$, the parameters are identical to A4 and A4$_{\rm core}$, respectively, but the stellar mass of the satellite is smaller $M_* = 1 \times 10^4 M_\odot$. These parameters correspond to the closest orbit where the tidal effects should be the largest. The other pair, B6 and B6$_{\rm core}$, uses $M_* = 1 \times 10^4\, M_\odot$ and the parameters of B3 and B3$_{\rm core}$, respectively. We do not use parameters of B4 for the reasons mentioned in the previous paragraphs. These cases are shown in the bottom panels of Figure 6. In the bottom left of this figure we notice that the inner mass of the satellite reduces due to the proximity to the disk's influence but the potential well is again deep enough to ensure the survival of the satellite. In the bottom right panel of the same figure we see that both cases B6 lead effectively to the same result; despite their low masses the satellites can remain with most of their initial mass after 10 Gyr. We point out that this is consistent with the arguments given above for B3$_{\rm core}$. In B6$_{\rm core}$ the satellite has a much smaller initial stellar mass concentrated within 1 kpc, thus fewer stars are stripped during its evolution and are insufficient to drag most of the central stars toward the outer regions as opposed to B3$_{\rm core}$. Nevertheless, we still observe a small effect of this process in this pair of simulations.

Indeed, comparing cases A and B, we note that for the cases in which orbits are far from the disk the density of the subhalo is a decisive parameter for determining the mass loss but has little influence in its survival. We found that the mass loss is greater if the subhalo has smaller density, but the dwarf galaxies still survive after 10 Gyr.

When the satellites have orbits close to the center of the host or when they strongly interact with the disk, the subhalo central density becomes an important factor for the survival and for the number of remaining satellites; this is consistent with previous works.

It is known that in CDM simulations, the satellites with cuspy subhalos can be stripped of stars but still survive as DM-only subhalos, which could be detected with gravitational lensing techniques. Here we show that if the satellites are in scalar field subhalos with central densities comparable to classical dSphs, some of their stars are stripped but the galaxies can survive with smaller masses and hence contribute to the number of dwarf satellites around an MW host. It must be noted that, in the SFDM model, the substructure is smaller due to the wave properties causing the cut-off in the power spectrum, as confirmed in Schive et al. (2014). Our result can

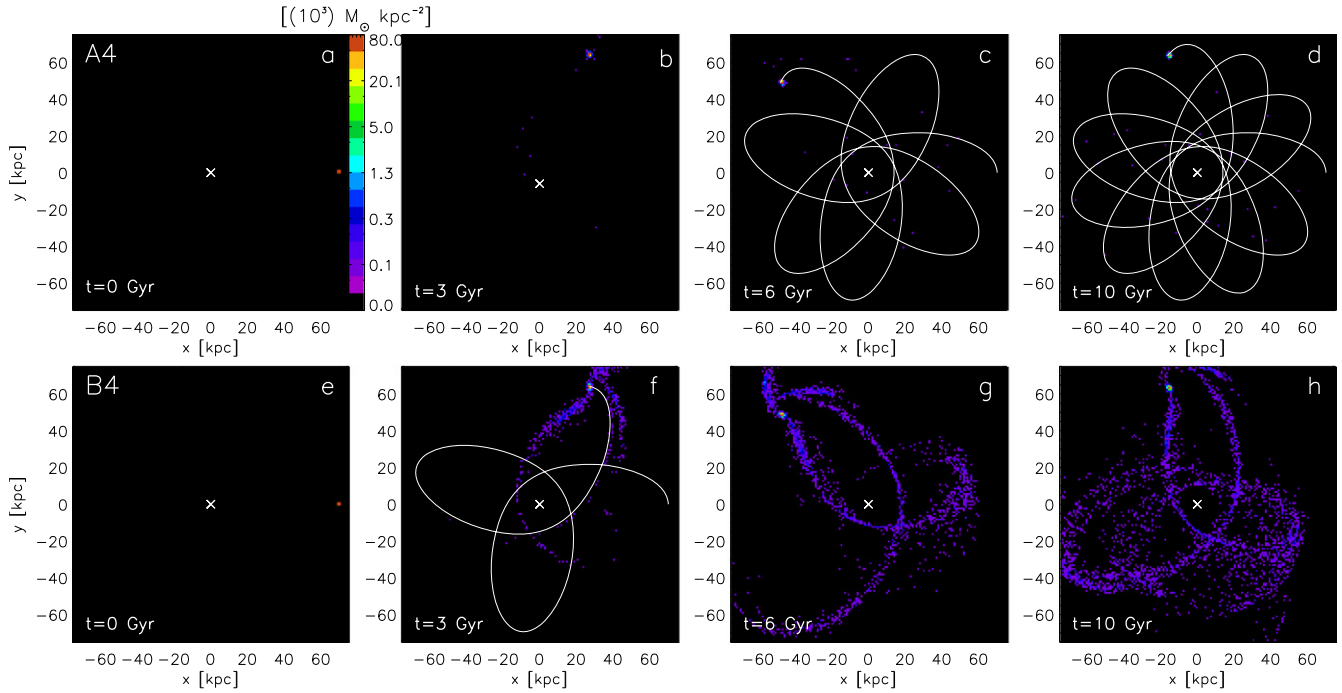

Figure 5. Surface mass density of the dwarf galaxy for $t = 0$, 3, 6, and 10 Gyr, for models A4 and B4 centered in the MW SFDM halo potential. The white cross shows the center of the MW, and the white line shows the dwarf's orbit around it.

Table 1
Parameters Used in Our Simulations

Simulation	$\frac{r_p}{r_a}$	Dwarf Orbit Plane	Dwarf ρ_0 $(10^7\,M_\odot\,(\mathrm{kpc})^{-3})$	MW ρ_0 $(10^7\,M_\odot\,(\mathrm{kpc})^{-3})$	MW Disk	DM Model
A1	1/2	x–y	16	1.91	…	SFDM
B1	1/2	x–y	3.1	1.91	…	SFDM
A2	1	x–y	16	1.91	✓	SFDM
B2	1	x–y	3.1	1.91	✓	SFDM
A3	1/2	x–y	16	1.91	✓	SFDM
$A3_{core}$	1/2	x–y	16	1.91	✓	Core
B3, B6[a]	1/2	x–y	3.1	1.91	✓	SFDM
$B3_{core}$, $B6_{core}$	1/2	x–y	3.1	1.91	✓	Core
A4, A6[b]	1/5	x–y	16	1.91	✓	SFDM
$A4_{core}$, $A6_{core}$	1/5	x–y	16	1.91	✓	Core
B4	1/5	x–y	3.1	1.91	✓	SFDM
$B4_{core}$	1/5	x–y	3.1	1.91	✓	Core
A5	1/5	45°	16	1.91	✓	SFDM
B5	1/5	45°	3.1	1.91	✓	SFDM

Note. Column 1 identifies the simulation, column 2 specifies r_p/r_a for the orbit, column 3 shows the plane of the orbit, the next two columns give the central density for the dwarf and the MW DM halos in each simulation, respectively, column 6 determines if a disk is present in the MW halo, and column 7 gives the DM model used in the simulation.

[a] Simulations B6 ($B6_{core}$) use the same parameters as B3 ($B3_{core}$) but with a satellite stellar mass $M_* = 1 \times 10^4\,M_\odot$.

[b] Simulations A6 ($A6_{core}$) use the same parameters as A4 ($A4_{core}$) but with a satellite stellar mass $M_* = 1 \times 10^4\,M_\odot$.

be tested with hydrodynamical SFDM cosmological simulations in the future.

For the lower density dwarfs (comparable to ultra faint dwarfs), we obtained that they could survive but only if their orbits do not get well inside the disks of their hosts. On the other hand, low density halos with close pericenter orbits can be fully stripped of stars if evolved for a long time even with a fixed subhalo potential, but as mentioned before we expect them to be destroyed once the fixed halo hypothesis is relaxed. Therefore, we do not get DM halos that are tiny and dark, contrary to the CDM predictions where the cusp prevents total disruption.

The formation of ultra faint dwarfs is still not clear but it is thought that they are the result of more massive dwarfs that were disrupted and left them as low density systems. We have seen that in the scenario of SFDM, depending on their distance to their host, these faint systems could also be produced from disrupted dwarfs with initial core profiles in the same way that they are when halos are assumed to have cusp profiles (Łokas et al. 2012).

Therefore, our results point to an alternative solution to the satellite overabundance problem and the cusp–core issue by means of the quantum DM properties of the scalar field without relying strongly on the messy astrophysical processes. Here, small mass subhalos with core profiles ($\rho(r) \sim r^0$) and with orbits not crossing the host's disk are able to survive for a long time; otherwise close encounters with the disk could completely destroy them. On the other hand, more massive dwarfs can get closer or farther from the host disk and still survive with core profiles. To determine the final fate of these galaxies and test the results from the present work, we will need simulations that involve the complexities of astrophysics, but we leave that for a future work.

From Equation (3) we see that for larger excited states the inner region becomes more compact and the halo core sizes can become smaller. In general a superposition of states may be present in an SFDM halo (Robles & Matos 2013a), however, Ureña-López & Bernal (2010) found that for a stable multi-state SFDM halo the number of bosons in excited states should decrease with increasing j, for instance, in a

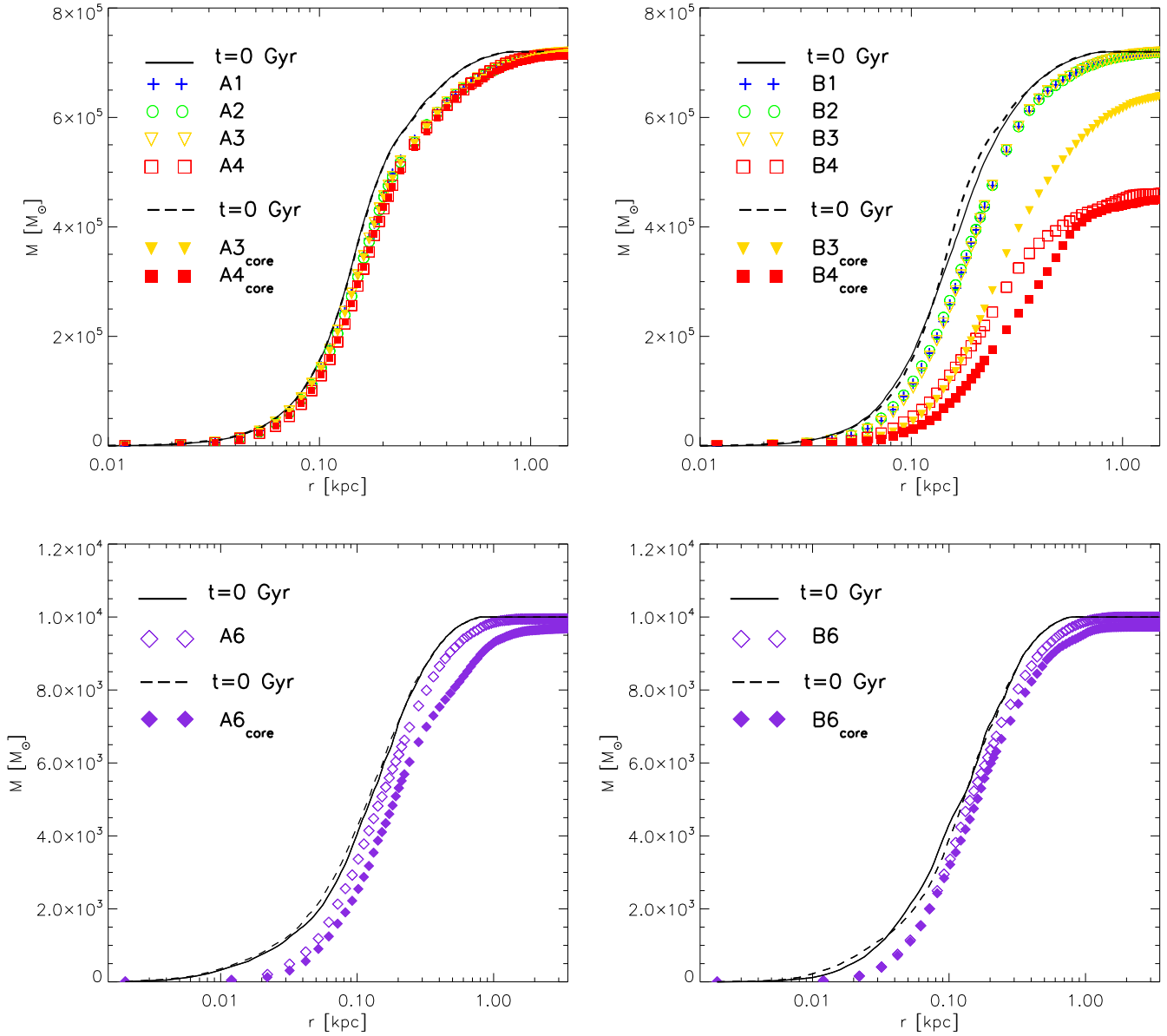

Figure 6. Upper panel: dwarf stellar mass for models A (left) and B (right) at $t = 0$ and $t = 10$ Gyr. The upper left panel would represent a classical dwarf and the upper right would be an ultra-faint-like galaxy. The different symbols in the panel represent the dark matter model used in that simulation according to Table 1. Bottom panels show small mass satellites with $M_* = 1 \times 10^4$ (models A6, A6$_{\rm core}$, B6, and B6$_{\rm core}$) at $t = 0$ and $t = 10$ Gyr; different symbols correspond to different simulations. In all A models of the SFDM the galaxy survives at the end of the simulation independent of the stellar mass and the orbits we considered; even the presence of a disk in the MW scalar field halo cannot destroy the satellite. In B models where the subhalo is less dense, the satellite loses more mass than in A cases but will still survive inside the subhalo, except when the pericenter becomes comparable to the disk's scalelength where we expect the scalar field subhalo to be disrupted too.

multi-state composed of the ground ($j = 1$) and first excited states ($j = 2$) the number of bosons in $j = 2$ should be less than or equal to those in $j = 1$ if the halo is to be stable, hence small core sizes are expected in massive galaxies, i.e., those where the SF ground state provides a poor description, depending on the required number of excited states in the halo, the halo core size can become smaller. Given that dwarf galaxies are consistent with halos with only $j = 1$, and from the stability constraint in the SFDM halos any contribution of higher energy states will be subdominant in such halos and the core sizes are dictated by the dominant ground state, being of $\sim$kpc for a boson mass of $\sim 10^{-22}\,{\rm eV}/c^2$. By fitting galaxies of different sizes it is possible to constrain the number of states in the SFDM halos required to agree with observations. As noted before, dwarfs seem to lie in ground state SFDM halos, while larger galaxies seem to require more than that, however, at this point it is unclear whether there is a mechanism that predicts the final superposition of a given SFDM halo; a statistical analysis fitting galaxies of different morphological types and sizes is required to derive such a relation.

Additionally, although we use a single state ($j = 4$) as a fit to the MW, we have not addressed its stability. Looking at the more general SFDM halo scenario mentioned above, it remains to be shown under what circumstances the inteplay of the different particle states within an SFDM halo, in our case an MW-like halo, can lead to a stable halo with a non-negligible fraction of bosons in a single state that extends to large radii;

this is something that needs to be addressed at a later time and will be vital to the viability of SFDM.

5. CONCLUSIONS

In this paper we explored within the context of the SFDM the influence that tidal forces have on a stellar distribution that is embedded in an SFDM halo with the distinctive feature of a flat central density. The satellite orbits around a dark matter halo with parameters that resemble those of the MW also modeled with a scalar field DM halo.

In general, the survival of a satellite depends on effects like its orbit, density, supernova explosions, its star formation history, and merger history in the case where a hierarchical model is assumed among other factors. Here we focused our analysis on the mass loss of a satellite galaxy hosted by a DM subhalo with two flat central density profiles: one that is predicted by the SFDM model as a consequence of the uncertainty principle, preventing the divergence of the central density, and the second profile which is a widely used empirical model, describing core-like mass distributions, frequently encountered in the literature. We explored different central densities for the halo and concentrated on the stellar evolution under various orbits and different stellar masses for both halo models.

Our results show that objects like Draco, with presumably large core sizes today, may have a simple explanation for their observed flat light distribution in the SFDM model because the stellar distribution remains bound even for tight orbits. A similar result was found in the context of CDM halos but on the condition of choosing more specific orbits (Wilkinson et al. 2004; Lux et al. 2010). Also, all galaxies in our A cases with core profiles survive for 10 Gyr. Thus dwarf galaxies that were accreted a long time ago will still persist as satellites with perhaps slightly smaller mass depending on the proximity of their orbits to their hosts. A comparison with the number of satellites is out of the scope of this work because for such a comparison we need to consider the uncertainties associated to specific details of the host formation and any recent major mergers that it could have had. Simulations addressing this issue would be desirable.

We also find a difference in the properties of the ultra faints; we showed that tidal disruption is also a mechanism for producing ultra faint dwarfs out of more massive dwarfs. Nevertheless the disruption does not produce a substantial change in the slope of the inner density profile. Therefore, even with the same mechanism used in CDM to form an ultra faint dwarf there is a stark difference with CDM halos in their final density slopes. In fact, while cores are a direct consequence in SFDM, CDM halos relied on effective supernovae feedback to form cores a long time ago, otherwise they are expected to retain their divergent mass profile which may be used to differentiate these models in the future.

Regarding the too-big-to-fail issue, to make a fair comparison with CDM simulations we will need a cosmological simulation that models the dark matter as a scalar field in order to study the number of the most massive halos around MW-sized hosts and determine if this represents a challenge in the SFDM model.

We think that further exploring the SFDM looks promising due to the possible natural solutions that it proposes to long-standing issues of the CDM model. Baryonic processes should be included in SFDM simulations as they can be more directly compared with observations.

T.M. thanks Joel Primack for helpful discussions. V.L. gratefully acknowledges support from the FRONTIER grant, and HB-L. The authors would like to thank the anonymous referee for insightful comments that helped increase the scope and improve the clarity of this paper. This work was supported in part by DGAPA-UNAM grant IN115311 and by CONACyT Mexico grant 49865-E. This work was partially supported by CONACyT México under grants CB-2009-01, no. 132400, CB-2011, no. 166212, and I0101/131/07 C-234/07 of the Instituto Avanzado de Cosmologia (IAC) collaboration (http://www.iac.edu.mx/). This work is supported by CONACyT Project no. 165584. Victor H. Robles is supported by a CONACYT scholarship.

REFERENCES

Agnello, A., & Evans, N. W. 2012, ApJL, 754, L39
Armandroff, T. E., Olszewski, E. W., & Pryor, C. 1995, AJ, 110, 2131
Belokurov, V., Walker, M. G., Evans, N. W., et al. 2010, ApJL, 712, L103
Berezhiani, Z. G., Sakharov, A. S., & Khlopov, M. Yu. 1992, SvJNP, 55, 1063
Bernal, A., Barranco, J., Alic, D., & Palenzuela, C. 2010, PhRvD, 81, 044031
Bonanos, A. Z., Stanek, K. Z., Szentgyorgyi, A. H., Sasselov, D. D., & Bakos, G. A. 2004, AJ, 127, 861
Boylan-Kolchin, M., Bullock, J. S., & Garrison-Kimmel, S. 2014, MNRAS, 443, L44
Boylan-Kolchin, M., Bullock, J. S., & Kaplinghat, M. 2011, MNRAS, 415, L40
Böhmer, C. G., & Harko, T. 2007, JCAP, 06, 025
Brook, C. B., Governato, F., Roškar, R., et al. 2011, MNRAS, 415, 1051
Charles, L. S., Speagle, J. S., Capak, P., et al. 2014, ApJL, 791, L25
Chavanis, P. H. 2012, A&A, 537, A127
Collins, C. A., Stott, J. P., Hilton, M., et al. 2009, Natur, 458, 603
Collins, M. L. M., Chapman, S. C., Rich, R. M., et al. 2014, ApJ, 783, 7
de Blok, W. J. G., Walter, F., Brinks, E., et al. 2008, AJ, 136, 2648
Diemand, J., Kuhlen, M., & Madau, P. 2007, ApJ, 657, 262
Diemand, J., Zemp, M., Moore, B., Stadel, J., & Corollo, C. M. 2005, MNRAS, 364, 665
Diez-Tejedor, A., Gonzalez-Morales, A. X., & Profumo, S. 2014, PRD, 90, 043517
Donnino, A., Schneider, A., Macciò, A. V., et al. 2013, JCAP, 03, 014
Feast, M., & Whitelock, P. 1997, MNRAS, 291, 683
Fellhauer, M., Kroupa, P., Baumgardt, H., et al. 2000, NewA, 5, 305
Finkelstein, S. L., Papovich, C., Dickinson, M., et al. 2013, Natur, 502, 524
Garrison-Kimmel, S., Boylan-Kolchin, M., Bullock, J. S., & Kirby, E. N. 2014a, MNRAS, 444, 222
Garrison-Kimmel, S., Boylan-Kolchin, M., Bullock, J. S., & Lee, K. 2014b, MNRAS, 438, 2578
Garrison-Kimmel, S., Rocha, M., Boylan-Kolchin, M., Bullock, J. S., & Lally, J. 2013, MNRAS, 433, 3539
Gentile, G., Salucci, P., Klein, U., Vergani, D., & Kalberla, P. 2004, MNRAS, 351, 903
Gilmore, G., Wilkinson, M. I., Wyse, R. F. G., et al. 2007, ApJ, 663, 948
Goerdt, T., Gnedin, O. Y., Moore, B., Diemand, J., & Stadel, J. 2007, MNRAS, 375, 191
González-Morales, A. X., Diez-Tejedor, A., Ureña-López, L. A., & Valenzuela, O. 2013, PhRvD, 87, 021301(R)
Governato, F., Brook, C., Mayer, L., et al. 2010, Natur, 463, 203
Governato, F., William, B., Mayer, L., et al. 2007, MNRAS, 374, 1479
Governato, F., Zolotov, A., Pontzen, A., et al. 2012, MNRAS, 422, 1231
Guzmán, F. S., & Matos, T. 2000, CQGra, 17, L9
Guzmán, F. S., & Ureña-López, L. A. 2006, ApJ, 645, 814
Harko, T., & Madarassy, E. J. M. 2011, JCAP, 01, 020
Hu, W., Barkana, R., & Gruzinov, A. 2000, PhRvL, 85, 1158
Ibata, R. A., Lewis, G. F., Conn, A. R., et al. 2014, Natur, 493, 62
Irwin, M., & Hatzidimitriou, D. 1995, MNRAS, 277, 1354
Kassin, S. A., Weiner, B. J., Faber, S. M., et al. 2012, ApJ, 758, 106
Klimentowski, J., Łokas, E. L., Kazantzidis, S., Mayer, L., & Mamon, G. A. 2009, MNRAS, 397, 2015
Klypin, A., Kravstov, A. V., Valenzuela, O., & Prada, F. 1999, ApJ, 522, 82

Łokas, E. L., Kazantzidis, S., & Mayer, L. 2012, ApJL, 751, L15
Lora, V., Grebel, E. K., Sánchez-Salcedo, F. J., & Just, A. 2013, ApJ, 777, 65
Lora, V., & Magaña, J. 2014, JCAP, 09, 011
Lora, V., Magaña, J., Bernal, A., Sánchez-Salcedo, F. J., & Grebel, E. K. 2012, JCAP, 02, 011
Lux, H., Read, J. I., & Lake, G. 2010, MNRAS, 406, 2312
Macciò, A. V., Paduroin, S., Anderhalden, D., et al. 2012, MNRAS, 424, 1105
Magaña, J., Matos, T., Robles, V. H., & Suárez, A. 2012a, JPhCS, 378, 012012
Magaña, J., Matos, T., Suárez, A., & Sánchez-Salcedo, F. J. 2012b, JCAP, 1210, 003
Marsh, D. J. E., & Silk, J. 2014, MNRAS, 437, 2652
Martin, N. F., de Jong, J. T. A., & Rix, H. W. 2008, ApJ, 684, 1075
Martinez-Medina, L. A., & Matos, T. 2014, MNRAS, 444, 185
Martinez-Medina, L. A., Robles, V. H., & Matos, T. 2015, PRD, 91, 023519
Mashchenko, S., Wadsley, J., & Couchman, H. M. P. 2008, Sci, 319, 174
Mateo, M., Olszewski, E. W., & Walker, M. G. 2008, ApJ, 675, 201
Matos, T., & Ureña-López, L. A. 2001, PhRvD, 63, 063506
Matos, T., & Ureña-López, L. A. 2007, GReGr, 39, 1279
McGaugh, S. S., & Milgrom, M. 2013, ApJ, 775, 139
McGaugh, S. S., Schombert, J. M., de Blok, W. J. G., & Zagursky, M. J. 2010, ApJL, 708, L14
Milgrom, M. 2010, in AIP Conf. Proc., 124, Invisible Universe (Melville, NY: AIP), 139
Miyamoto, M., & Nagai, R. 1975, PASJ, 27, 533
Moore, B., Ghigna, S., Governato, F., et al. 1999, ApJL, 524, L19
Muñoz, R. R., Frinchaboy, P. M., Majewski, S. R., et al. 2005, ApJL, 631, L137
Navarro, J. F., Frenk, C. S., & White, S. D. M. 1997, ApJ, 490, 493
Navarro, J. F., Ludlow, A., Springel, V., et al. 2010, MNRAS, 402, 21
Odenkirchen, M., Grebel, E. K., Harbeck, D., et al. 2001, AJ, 122, 2538
Oh, S. H., de Block, W. J. G., Brinks, E., & Kennicut, R. C. 2008, AJ, 136, 2761
Okamoto, T., Gao, L., & Theuns, T. 2008, MNRAS, 390, 920
Peñarrubia, J., Benson, A. J., Walker, M. G., et al. 2010, MNRAS, 406, 1290
Peñarrubia, J., Pontzen, A., Walker, M. G., & Koposov, S. E. 2012, ApJL, 759, L42
Plummer, H. C. 1911, MNRAS, 71, 460
Pontzen, A., & Governato, F. 2012, MNRAS, 421, 3464
Rashkov, V., Madau, P., Kuhlen, M., & Diemand, J. 2012, ApJ, 745, 142
Read, J. I., Wilkinson, M. I., Evans, N. W., Ginlmore, G., & Kleyna, J. T. 2006, MNRAS, 367, 387
Robles, V. H., & Matos, T. 2012, MNRAS, 422, 282
Robles, V. H., & Matos, T. 2013a, ApJ, 763, 19
Robles, V. H., & Matos, T. 2013b, PhRvD, 88, 083008
Rocha, M., Peter, A. H. G., Bullock, J. S., et al. 2013, MNRAS, 430, 81
Salucci, P., Wilkinson, M. I., Walker, M. G., et al. 2012, MNRAS, 420, 2034
Scannapieco, C., Thacker, R. J., & Davis, M. 2001, ApJ, 557, 605
Scannapieco, C., Wadepuhl, M., Parry, O. H., et al. 2012, MNRAS, 423, 1726
Schive, H. Y., Chiueh, T., & Broadhurst, T. 2014, NatPh, 10, 496
Simon, J. D., & Geha, M. 2007, ApJ, 670, 313
Sin, S. J. 1994, PhRvD, 50, 3650
Strigari, L. E., Bullock, J. S., Kaplinghat, M., et al. 2006, ApJ, 652, 306
Strigari, L. E., Frenk, C. S., & White, S. D. M. 2014, arXiv:1406.6079
Suárez, A., & Matos, T. 2011, MNRAS, 416, 87
Suárez, A., Robles, V. H., & Matos, T. 2014, in Astrophysics and Space Science Proc., 38, Accelerated Cosmic Expansion (Berlin: Springer), 107
Tollerud, E. J., Beaton, R. L., Geha, M., et al. 2012, AAS, 219, 20104
Trachternach, C., de Block, W. J. G., Walter, F., Brinks, E., & Kennicut, R. C. 2008, AJ, 136, 2720
Ureña-López, L. A., & Bernal, A. 2010, PRD, 82, 123535
Walker, M. G., Mateo, M., & Olszewski, E. W. 2009, AJ, 137, 3100
Walker, M. G., & Peñarrubia, J. 2011, ApJ, 742, 20
Wilkinson, M. I., Kleyna, J. T., Evans, N. W., et al. 2004, ApJL, 611, L21
Wolf, J., Martinez, G. D., Bullock, J. S., et al. 2010, MNRAS, 406, 1220